

SANS Studies on Frozen Inhomogeneities and Local Structure in Polymer Gels

Mitsuhiro SHIBAYAMA*, Tomohisa NORISUYE and Fumiyoshi IKKAI**

*Department of Polymer Science and Engineering, Kyoto Institute of
 Technology, Matsugasaki, Sakyo-ku, Kyoto 606-8585, Japan*

The structure factor $S(q)$ for a series of poly(*N*-isopropylacrylamide-*co*-acrylic acid) (NIPA/AAc) copolymer gels having different cross-link concentrations has been investigated by small-angle neutron scattering for a wide range of scattering vector, q . The range of q was covered to be $0.07 \leq q \leq 6 \text{ nm}^{-1}$ by measuring $S(q)$ with three different sample-to-detector distances, i.e., 1, 5, and 15.3 m. This allowed a quantitative analysis of the interaction parameters both at gel preparation and at observation. A positive deviation of the scattered intensity at low q -region was observed and was explained by additional built-in inhomogeneities and by chain-entanglement effects introduced during the process of gel formation. A positive deviation was also found at the large- q limit, which was interpreted as an increase in the local chain rigidity by introduction of crosslinks.

KEYWORDS: polymer gels, structure factor, inhomogeneities, chain-entanglements, local chain rigidity

§1. Introduction

Due to topological constraints introduced by crosslinks, polymer gels have two types of concentration fluctuations; thermal fluctuations and frozen inhomogeneities. The frozen inhomogeneities are inherent in polymer gels, and depend not only on the state of observation but also on the state of preparation.^{1–3)} If a gel is partially charged, the structure factor, $S(q)$, becomes even more sophisticated due to participation of Debye-Hückel interaction, where q is the scattering vector. The structure factor is similar to that of non-charged polymer gels if the solvent is good enough to the network polymer chains. However, when the solvent becomes poor, a distinct scattering maximum appears in the structure factor as a result of microphase separation. This is due to compensation of high penalty of localization of charges and macroscopic demixing.⁴⁾ In the previous papers, we discussed the structure factor of weakly charged polymer gels as a function of temperature,⁵⁾ polymer concentration,⁶⁾ pH⁷⁾ and the degree of stretching.⁸⁾ Although a good agreement between the experimental and theoretical structure factors^{4,9)} was obtained, it was not conclusive because of the limitation of the q -range. A typical q -range was $0.1 \leq q \leq 1 \text{ nm}^{-1}$, which was not enough for a quantitative comparison of experimental and theoretical scattering functions. In this paper, we extended the experimental q region to $0.07 \leq q \leq 6 \text{ nm}^{-1}$, and compared the experimental $S(q)$ s with theoretical scattering functions proposed by Rabin-Panyukov (RP).⁹⁾ We restricted our discussion only for $S(q)$ s at room temper-

ature where no significant charge effects appear. This allowed us to reduce the number of fitting parameters related to charges. Analyses of $S(q)$ for weakly charged gels in the poor solvent regime will be reported in the forthcoming paper.

§2. Theoretical Section

Recently, Panyukov and Rabin developed a comprehensive statistical theory for polymer gels, which takes into account the contribution of frozen inhomogeneities built-in by crosslinking polymer chains.^{2,10)} The structure factor consists of two contributions, one from thermal fluctuations, $G(q)$ (the dynamic correlator), and the other from static density inhomogeneities, $C(q)$ (the static correlator);

$$S(q) \equiv \overline{\langle \rho(q)\rho(-q) \rangle} = G(q) + C(q) \quad (2.1)$$

$$G(q) \equiv \langle \rho(q)\rho(-q) \rangle = \langle \rho^{\text{th}}(q)\rho^{\text{th}}(-q) \rangle \quad (2.2)$$

$$C(q) \equiv \overline{\rho^{\text{eq}}(q)\rho^{\text{eq}}(-q)} \quad (2.3)$$

where $\rho^{\text{eq}}(q)$, $\rho^{\text{th}}(q)$, and $\rho(q)$ are the Fourier components of the equilibrium density variations, of the thermal density fluctuations, and of the total density variations, respectively. Thus,

$$\rho(q) \equiv \rho^{\text{eq}}(q) + \rho^{\text{th}}(q) \quad (2.4)$$

Figure 1 schematically shows the two types of concentration fluctuations and two types of averages; the structure (ensemble) average denoted by \overline{X} and the thermal average given by $\langle X \rangle$, respectively, where $\rho(q)$ is the Fourier component of the density variation. Note

* Present address: Neutron Scattering Laboratory, The Institute for Solid State Physics, The University of Tokyo, Tokai, Naka-gun, Ibaraki 319-1106, Japan.

** Present address: The Institute of Advanced Science Research, L'ORÉAL Tsukuba Center, 5-5 Tokodai, Tsukuba, Ibaraki 300-2635, Japan.

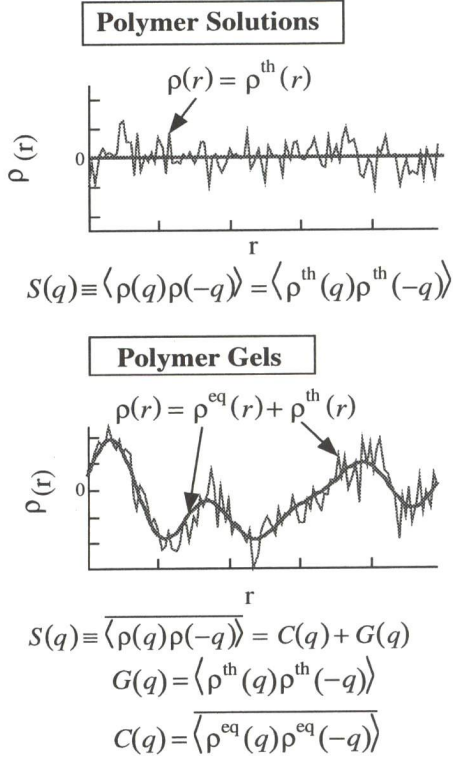


Fig. 1. Schematic representation showing the two types of concentration fluctuations, $\rho^{\text{eq}}(r)$, and $\rho^{\text{th}}(r)$, where r is the space coordinate.

that $\rho^{\text{eq}}(q)$ minimizes the free energy of the gel and has the following properties; $\langle \rho^{\text{eq}}(q) \rangle \neq 0$ and $\overline{\rho^{\text{eq}}(q)} = 0$. Rabin and Panyukov (RP) generalized the theory for weakly charged gels by incorporating a q -dependent interaction parameter $w(q)$.⁹⁾ $G(q)$ and $C(q)$ are given by

$$G(q) = \frac{\phi N g(q)}{1 + w(q)g(q)} \quad (2.5)$$

$$C(q) = \frac{\phi N}{[1 + w(q)g(q)]^2 (1 + Q^2)^2} \times \left[6 + \frac{9}{w_0(q) - 1 + Q^2(\phi_0/\phi)^{2/3}/2} \right] \quad (2.6)$$

where N , ϕ , and ϕ_0 denote the average number of segments between cross-linking points, the polymer volume fractions at observation and at preparation, respectively. Q is defined as the dimensionless wave vector by,

$$Q = aN^{1/2}q/\sqrt{6} \quad (2.7)$$

where a is the Kuhn segment length. It should be noted here that $G(q)$ and $C(q)$ are coupled with the function $g(q)$, which is given by

$$g(q) = \frac{1}{Q^2/2 + (4Q^2)^{-1} + 1} + \frac{2(\phi/\phi_0)^{2/3}}{(1 + Q^2)^2} \quad (2.8)$$

Here, $g(q)$ represents the structure factor of a sub-chain between crosslinks. The effect of crosslinks appears in

the second term in the denominator of the first term of the RHS in Eq. 2.8.¹¹⁾ $g(q)$ also contains information at which concentration the gel is made, i.e., ϕ_0 in the second term of the RHS in Eq. 2.8. The effect of charges appears in the dimensionless net-excluded volume parameters, $w(q)$ and $w_0(q)$ which are q -dependent,

$$w_q = (1 - 2\chi + \phi)\phi N + \frac{l_B f^2 \phi N^2}{Q^2 + l_B(f + 2C_S)\phi N} \quad (2.9)$$

$$w_0(q) = (1 - 2\chi_{\text{prep}} + \phi_0)\phi_0 N + \frac{\hat{l}_B f_0^2 \phi_0 N^2}{Q^2(\phi_0/\phi)^{2/3} + \hat{l}_B f_0 \phi_0 N} \quad (2.10)$$

where \hat{l}_B is the dimensionless Bjerrum length defined by

$$\hat{l}_B = 4\sqrt{6}\pi l_B/a \quad (2.11)$$

and χ is the Flory-Huggins interaction parameter. l_B is the Bjerrum length (≈ 0.7 nm for aqueous solutions at 25 °C). f and f_0 are the degree of ionization at observation and at preparation, respectively, and C_S is the salt concentration added in the observation state. Although the RP theory has many parameters, in principle, most of them can be fixed by the experimental condition, particularly for the parameters at preparation, e.g., ϕ_0 , f_0 , and N , and some at observation, e.g., ϕ and f . Therefore, a curve fitting of an observed intensity function $I(q)$ with the theoretical structure factor $S(q)$ can be carried out with a few numbers of floating parameters, e.g. χ and the intensity scale factor, K_N , where

$$I(q) = K_N S(q) \quad (2.12)$$

The intensity scale factor can be calculated if $I(q)$ is obtained in the absolute intensity scale. In this case, K_N is given by¹²⁾

$$K_N = \frac{N_A}{v_B} \left[b_A \left(\frac{v_B}{v_A} \right) - b_B \right]^2 \quad (2.13)$$

where N_A is the Avogadro's number, and v_i and b_i are the molar segment volume and the scattering length of the component i , respectively.

§3. Experimental Section

Samples Mixtures of N -isopropylacrylamide (NIPA) and acrylic acid (AAc) monomers with the ratio of NIPA/AAc = 636 mM / 64 mM were dissolved in 40 mL of D₂O including 20 mg of ammonium persulfate (polymerization initiator). Each solution was divided into eight vessels with equal amounts and then the given amounts of N,N' -methylenebisacrylamide (BIS; cross-linker) were added to each solution. Then, the solutions were filtered with a 0.2 mm micropore filter. Gelation was initiated in a test tube thermostatted at 20 °C by adding 24 mL of N,N,N',N' -tetramethylethylenediamine (TEMED; accelerator). The final concentrations of BIS, C_{BIS} , were 0, 2, 4, 6, 8, 16, and 24 mM. The obtained transparent gels were sifted by a 500 μm sieve to small pieces in order

to obtain quick thermal equilibration upon a change of temperature. The smashed gels were sealed in a brass cell with a pair of quartz windows and a rubber O-ring. Thus sealed gels were used for SANS experiments without further treatment. The sample thickness was 2 mm. Another set of NIPA/AAc gels with the same recipe was prepared in a test tube for light scattering experiment.

SANS Small-angle neutron scattering (SANS) measurements were performed on the 30 m-SANS facility (NG7) at National Institute of Standards and Technology, Maryland, USA. The cells containing gel samples were irradiated by a neutron beam with the wavelength of 0.9 nm. Scattered neutrons were counted with an area detector and were circularly averaged by taking account of the detector inhomogeneities. Then, $I(q)$ in the absolute intensity scale was obtained by scaling after the correction for cell scattering, fast neutrons, transmission, and incoherent scattering. Here, the scattering profiles were obtained at three sample-detector-distances (SDD), i.e., at 1 m (which covered the range of $0.6 \leq q \leq 6 \text{ nm}^{-1}$), 5 m ($0.15 \leq q \leq 1 \text{ nm}^{-1}$), and 15.3 m ($0.07 \leq q \leq 0.2 \text{ nm}^{-1}$), from which a master curve for $I(q)$ was constructed with a wide range of q , i.e., $0.07 \leq q \leq 6 \text{ nm}^{-1}$.

LS Light scattering (LS) experiments were carried out on a laboratory-made dynamic light scattering instrument with a 10 mW He-Ne laser (wavelength, $\lambda = 632.8 \text{ nm}$) coupled with a photon correlator (DLS-7, Otsuka Electric Co.). The details of the instrument were described elsewhere.¹³ The test tube (the inner diameter, $d = 10 \text{ mm}$) containing a gel was placed in the silicon oil bath whose temperature was controlled within an error of $\pm 0.1 \text{ }^\circ\text{C}$. The light scattered intensity, $I(q_{\text{LS}})$, was measured at a fixed scattering angle of 60° . The scattering vector was $q_{\text{LS}} \simeq 1.31 \times 10^{-2} \text{ nm}^{-1}$ ($= (4n\pi/\lambda)\sin(\theta/2)$), where n is the refractive index of water. The ensemble average of the scattered intensity, $\langle I(q_{\text{LS}}) \rangle_{\text{E}}$, in the units of count per second (cps) was calculated by measuring $I(q_{\text{LS}})$ s at 100 different sample positions chosen arbitrarily in the gel.

§4. Results and Discussion

Figure 2 shows the variation of $\langle I(q_{\text{LS}}) \rangle_{\text{E}}$ with crosslinker concentration, C_{BIS} . The inset shows the variation of $I(q_{\text{LS}})$ with sample position. As shown in the inset, $I(q_{\text{LS}})$ strongly fluctuates with sample position for $C_{\text{BIS}} = 24 \text{ mM}$. This is due to nonergodicity of the system.¹⁴ The horizontal line indicates the ensemble average intensity, $\langle I(q_{\text{LS}}) \rangle_{\text{E}}$. It is clear that $\langle I(q_{\text{LS}}) \rangle_{\text{E}}$ increases with C_{BIS} . It is demonstrated elsewhere that $\langle I(q) \rangle_{\text{E}}$ can be decomposed to the dynamic ($\sim G(q)$) and static components ($\sim C(q)$) by employing dynamic light scattering technique.^{15,16}

Figure 3 shows the scattered intensity functions, $I(q)$, for poly-NIPA/AAc solutions ($C_{\text{BIS}} = 0 \text{ mM}$) and gels ($C_{\text{BIS}} = 2, 4, 6, 8, 16, 24 \text{ mM}$) obtained by SANS. In order to avoid overlap, a vertical offset with an increment of $+0.5$ was added (in the logarithmic scale) to each $I(q)$ with respect to that of NIPA/AAc solution. It is clear that $I(q)$ for $q < 1 \text{ nm}^{-1}$ has strong C_{BIS} dependence,

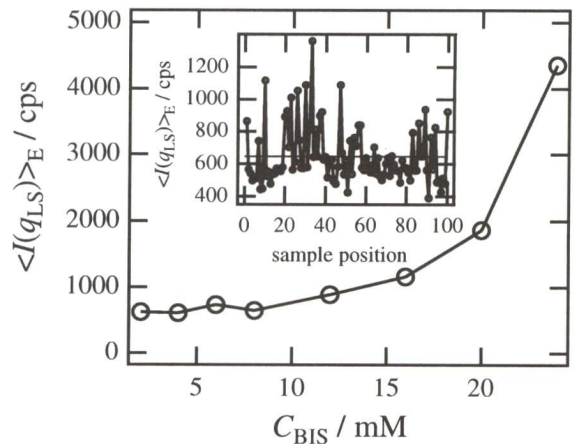


Fig. 2. Crosslinker Concentration, C_{BIS} , dependence of the ensemble average scattered intensity, $\langle I(q_{\text{LS}}) \rangle_{\text{E}}$. The inset shows an example of speckle pattern.

and $I(q)$ increases with increasing C_{BIS} . The asymptotic behavior of $I(q)$ for $q > 1 \text{ nm}^{-1}$ is also different whether or not the system is crosslinked. In order to analyze the structure factor, a curve fitting of $I(q)$ was carried out with the RP theory.

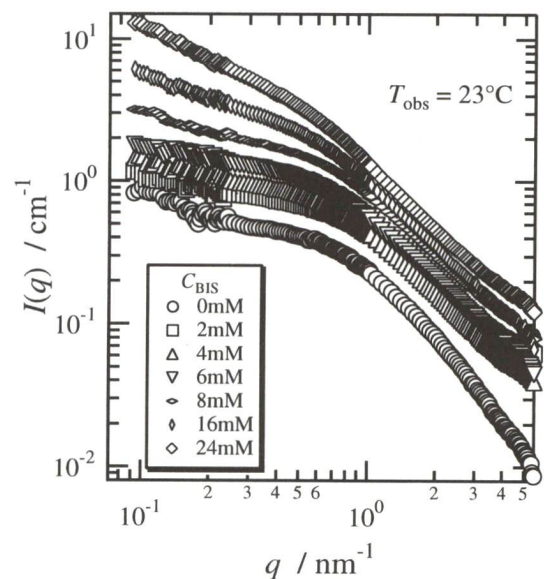


Fig. 3. SANS intensity functions for NIPA/AAc solution and gels prepared with different C_{BIS} 's. Each set of data is vertically shifted with the offset of $+0.5$ with respect to the solution data in order to avoid overlap.

Figure 4 shows an example of curve fitting for the cases of NIPA/AAc ($C_{\text{BIS}} = 0 \text{ mM}$) and NIPA/AAc ($C_{\text{BIS}} = 24 \text{ mM}$). The solid symbols indicate the results obtained with the 5-m collimation. The presence of data at low ($q \leq 0.2 \text{ nm}^{-1}$) and high q ($q \geq 1 \text{ nm}^{-1}$) enabled us to a quantitative analysis of scattered intensity functions. First of all, it should be noted that even for the polymer solution ($C_{\text{BIS}} = 0 \text{ mM}$), an upturn in $I(q)$ was observed for $q < 0.2 \text{ nm}^{-1}$. This indicates that frozen inhomogeneities are also present in polymer solutions. Frozen

inhomogeneities in a polymer solution are often observed if the solution is highly viscous and/or has specific molecular interactions, such as hydrophobic interaction. Since the volume fraction of the polymer network at preparation was known and it was unchanged at observation, we set $\phi = \phi_0 = 0.079$. The segment length is known to be $a = 0.812$ nm. In the case of the polymer solution, the scattered intensity is solely given by $G(q)$, which is rewritten by taking the large- q limit,

$$G(q) = \left[\frac{a^2 q^2}{12\phi} + \frac{w(q)}{\phi N} \right]^{-1} \quad (4.1)$$

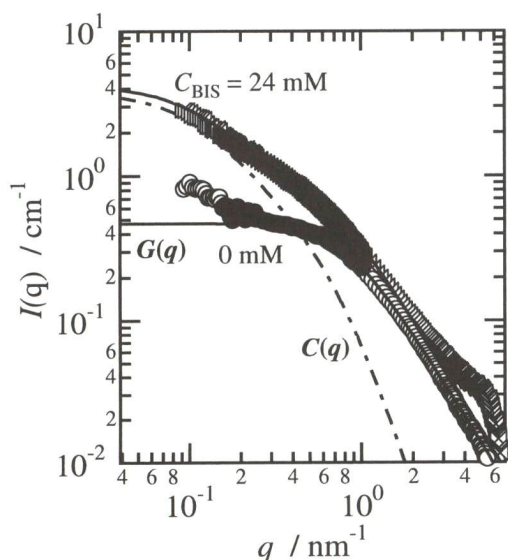


Fig. 4. Example of curve fitting. NIPA/AAc solution ($C_{\text{BIS}} = 0$ mM) and NIPA/AAc gel ($C_{\text{BIS}} = 24$ mM). $I(q)$ of the gel is decomposed to $G(q)$ and $C(q)$. The solid symbols indicate the result obtained with the 5 m collimation.

The result is shown by the solid line with the symbol of $G(q)$. The interaction parameter at observation ($T = 23^\circ \text{C}$) was estimated to be $\chi = 0.413$ from this fit. Note that Eq. 4.1 is analogous to the so-called Ornstein-Zernike function,

$$S_{\text{OZ}}(q) \sim \frac{1}{1 + \xi^2 q^2} \quad (4.2)$$

where ξ is the correlation length. As a matter of fact, ξ was evaluated to be 1.3 nm for the case of $C_{\text{BIS}} = 0$ mM, which is in good agreement with the value reported elsewhere.¹⁷⁾ In the case of polymer gels, the information of the interaction parameter at sample preparation is stored in $S(q)$. Hence, by curve fitting of the scattered intensity for NIPA/AAc ($C_{\text{BIS}} = 24$ mM) with the assumption of χ for the gel being equal to that of the polymer solution, we estimated $\chi_0 = 0.455$ and the degree of polymerization between crosslinks $N = 92.2$. The dash-dot line indicates $C(q)$ for NIPA/AAc ($C_{\text{BIS}} = 24$ mM).

By using these parameters, all of the scattered intensity functions were fitted with the theory as shown by the solid lines in Fig. 5. The fitting parameters employed

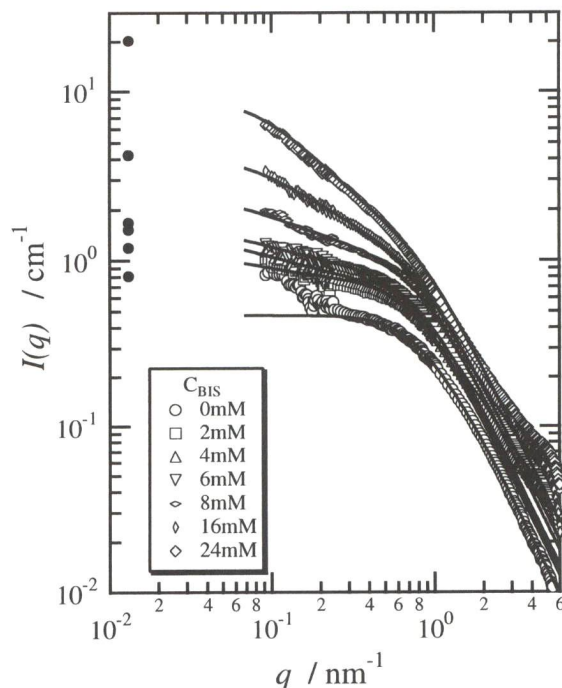


Fig. 5. Results of curve fitting (the solid lines). Data are vertically shifted with the offset of 0.5. Solid circles indicate $\langle I(q_{\text{LS}}) \rangle_{\text{E}}$.

here are the scaling factor, K_{N} , and the degree of polymerization between crosslinks, N . Although the K_{N} is supposed to be constant, it had to be floated about 10 % in order to account for minor errors arising from the evaluation of the sample thickness and transmission. This is due to the fact that the sample thickness could not be precisely determined because of the use of smashed gels. Note that the smashed gels were used in order to fasten the response of thermal equilibration. The solid circles at $q = 1.31 \times 10^{-2} \text{ nm}^{-1}$ indicate the ensemble average light scattered intensity, $\langle I \rangle_{\text{E}}$, which is supposed to be proportional to $I(q)$. Here, the set of $\langle I \rangle_{\text{E}}$'s was shifted vertically in order to match the scattered intensity functions obtained by SANS. As shown here, $\langle I \rangle_{\text{E}}$'s are located more or less on the extrapolated lines of $I(q)$'s, indicating that the frozen inhomogeneities observed by LS and SANS are the same. The fitted values of N by the RP theory are increasing function of C_{BIS} as is expected. Figure 6 shows the variation of N with

$$N_{\text{calc}} = (C_{\text{NIPA}} + 2C_{\text{BIS}}) / 2C_{\text{BIS}}$$

The deviation from the linear relationship between N and N_{calc} is ascribed to chain entanglement effect.

Another interesting feature is the asymptotic behavior in $I(q)$ at large q values. As shown in the figure, $I(q)$ has a power law behavior, $I(q) \sim q^{-s}$, where s is the scattering exponent. Eq. 4.1 and 4.2 predict $s = 2$ and it is well known that s can be 5/3 for polymer solutions in a good solvent. The extension of the experimental q range allowed us to examine this exponent for polymer solutions ($C_{\text{BIS}} = 0$ mM) and gels ($C_{\text{BIS}} = 2 \sim 24$ mM). Surprisingly, s changes from 2 to 1.4 by introduction of

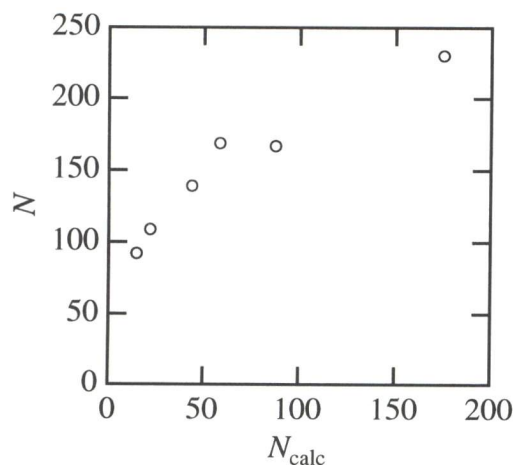


Fig.6. Variation of the number of segments between crosslinks evaluated by the fit, N , as a function of the calculated value, N_{calc} .

crosslinks as shown in Fig. 7. This change cannot be explained by the solvent nature. One possible explanation is that the local chain-rigidity increases by crosslinking, leading to a lowering of s .

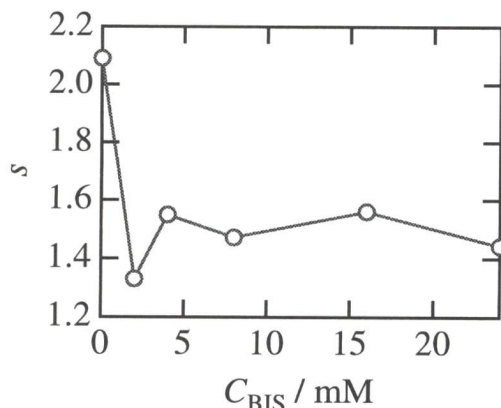


Fig.7. Variation of the scattering exponent s as a function of C_{BIS}

§5. Conclusion

The structure factors, $I(q)$, for weakly charged polymer gels and the corresponding polymer solution were analyzed as a function of crosslink density. In the case of polymer solution, the structure factor was well represented by an Ornstein-Zernike type function from which

the correlation length, ξ , was estimated to be 1.3 nm. The asymptotic behavior of the structure factor at high q region was scaled to be $I(q) \sim q^{-2}$, indicating that the polymer chain in the blob characterized by ξ is more or less in the unperturbed state. In the case of gels, a significant contribution of frozen inhomogeneities appears at low q values and it increases with increasing crosslink density. In addition, $I(q) \sim q^{-1.4}$ was obtained, which may indicate an increase in chain rigidity in the blob by crosslinking. The analysis on the structure factor disclosed that the structure factor of crosslinked systems is governed by not only by the chemical crosslinks but also by entanglements.

Acknowledgements

This work is partially supported by the Ministry of Education, Science, Sports and Culture, Japan (Grant-in-Aid, 12450388 to M.S.). Thanks are due to the Cosmetology Research Foundation, Tokyo, for financial assistance. F.I. and T.N. acknowledge the Research Fellowship of the Japan Society for the Promotion of Science for Young Scientists. F.I. is also grateful to the National Institute of Standards and Technology, Gaithersburg, MD, for giving a chance to stay as a guest researcher.

- 1) P. G. de Gennes, *Scaling Concepts in Polymer Physics* (Cornell University, Ithaca, 1979).
- 2) S. Panyukov and Y. Rabin: *Physics Report* **269** (1996) 1.
- 3) M. Shibayama, : *Macromol. Chem. Phys.* **199** (1998) 1.
- 4) V. Borue and I. Erukhimovich: *Macromolecules* **21** (1988) 3240.
- 5) M. Shibayama, T. Tanaka, and C. C. Han: *J. Chem. Phys.* **97** (1992) 6829.
- 6) M. Shibayama, T. Tanaka, and C. C. Han: *J. Chem. Phys.* **97** (1992) 6842.
- 7) M. Shibayama, F. Ikkai, S. Inamoto, S. Nomura and C. C. Han: *J. Chem. Phys.* **105** (1996) 4358.
- 8) M. Shibayama, K. Kawakubo, F. Ikkai, and M. Imai: *Macromolecules* **31** (1998) 586.
- 9) Y. Rabin and S. Panyukov: *Macromolecules* **30** (1997) 301.
- 10) S. Panyukov and Y. Rabin: *Macromolecules* **29** (1996) 7960.
- 11) P. G. de Gennes: *J. Phys. Lett.* **40** (1979) 545.
- 12) J. S. Higgins and H. C. Benoit: *Polymers and Neutron Scattering* (Clarendon Press, Oxford, 1994).
- 13) M. Shibayama, T. Takeuchi, and S. Nomura: *Macromolecules* **27** (1994) 5350.
- 14) P. N. Pusey and W. van Megen: *Physica A* **157** (1989) 705.
- 15) J. G. H. Joosten, J. L. McCarthy, and P. N. Pusey: *Macromolecules* **24** (1991) 6690.
- 16) M. Shibayama, T. Norisuye, and S. Nomura: *Macromolecules* **29** (1996) 8746.
- 17) M. Shibayama and T. Tanaka: *J. Chem. Phys.* **102** (1995) 9392.